DOI: 10.1002/chem.201002821

Starburst Triarylamine Donor–Acceptor–Donor Quadrupolar Derivatives Based on Cyano-Substituted Diphenylaminestyrylbenzene: Tunable Aggregation-Induced Emission Colors and Large Two-Photon Absorption Cross Sections

Bing Wang,[a] Yaochuan Wang,[b] Jianli Hua,*[a] Yihua Jiang,[a] Jinhai Huang,[a] Shixiong Qian,[b] and He Tian*[a]

Abstract: In this work, we have developed a new class of aggregation-induced emission (AIE) active compounds, in which three electron-donating diphenylamine, phenothiazine, or carbazole groups are connected to the 1, 4-positions of the benzene through bis(α-cyano-4-diphenylaminostyryl) conjugation bridges to form three triarylamine quadrupolar derivatives (**3a**–**c**). Their one- and two-photon absorption properties have been investigated. The two-photon absorption (2PA) cross sections measured by the open-aperture Z-scan technique were determined to be 1016, 1484, and 814 GM for **3a**–**c**, respectively. From this result, the high 2PA properties of these molecules are attributed to the extended π system and enhanced intramolecular charge transfer from the starburst triarylamine to the cyano group. Moreover, cyano-substituted diphenylamine styrylbenzene (CNDPASB)-based compounds are very weakly fluorescent in THF, but their intensities increase by almost 230, 70, and 5 times, respectively, in water/THF (v/v 90%) mixtures, in which they exhibit strongly enhanced red, orange, and deep yellow fluorescence emissions, respectively. This result indicates that the intramolecular vibration and rotation of these dyes is considerably restricted in nano-aggregates formed in water, leading to significant increases in fluorescence. It was found that the color tuning of the CNDPASB-based compounds could be conveniently accomplished by changing the starburst triarylamine donor moiety. Multilayer electroluminescence devices with TPBI (2,2′,2″-(benzene-1,3,5-triyl)-tri(1-phenyl-1*H*-benzimidazole)) electron-transporting layers have been made, with **3a** and **3c** as a non-doping red–yellow emitter. The preliminary results for these multilayer devices show a maximum efficiency of 0.25%, and electroluminescence (EL) wavelengths around 568 nm. The excellent 2PA and AIE properties of these compounds make them potential materials for biophotonic applications.

Keywords: aggregation · electrochemistry · fluorescence · organic light-emitting diodes · triarylamines · two-photon absorption

Introduction

Materials displaying high two-photon absorption (2PA) have attracted considerable interest recently, owing to their potential application in two-photon dynamic therapy,[1] three-dimensional optical data storage,[2] up-converted lasing,[3] optical power limiting materials,[4] bioimaging,[5] and so forth. For the full exploitation of the great potential of the 2PA process, the strategy for the design of molecules with large 2PA cross sections (σ) has been investigated both experimentally and theoretically.[6,7] The designs include symmetrical donor–conjugated-bridge–donor (D-π-D), acceptor–conjugated-bridge–acceptor (A-π-A) and donor–conjugated-bridge–acceptor–conjugated-bridge–acceptor–conjugated-bridge–donor (D-π-A-π-A-π-D), or asymmetrical donor–conjugated-bridge–acceptor (D-π-A) arrangements. The enhancement of σ has been correlated with intramolecular charge transfer from the terminal donor groups to the π bridge.[8] In addition, the magnitude of σ can be controlled through the modification of the molecular structure in such a way as to affect the amount of intramolecular charge transfer. Specifically, σ increases when the conjugation length of the π system is increased, and when electron acceptors (A) are attached as side groups to the π bridge, to form molecules of general structure D-A-D.[9] Many efforts have been made to develop novel 2PA materials by the modification of D/A groups or branching symmetry. Currently, 2PA materials with multibranched triarylamine are attracting great interest, and have become the focus of in-

[a] B. Wang, Prof. Dr. J. Hua, Y. Jiang, J. Huang, Prof. Dr. H. Tian
Key Laboratory for Advanced Materials
Institute of Fine Chemicals and Department of Chemistry
East China University of Science and Technology
130 Meilong Road, Shanghai 200237 (P.R. China)
Fax: (+86) 21-64252758
Fax: (+86) 21-64252756
E-mail: jlhua@ecust.edu.cn
tianhe@ecust.edu.cn

[b] Dr. Y. Wang, Prof. Dr. S. Qian
Department of Physics, Fudan University
Shanghai 200433 (P.R. China)

tensive research in the area of 2PA materials for their good electron-donating and transporting capabilities,[10] which can enhance the 2PA cross section owing to the increase in chromophore density.[11,12]

Many dyes with large 2PA were designed and synthesized. However, most of 2PA dyes are hydrophobic, and their fluorescence is often quenched on aggregation, although they may show high fluorescence efficiency in solutions, which greatly limits their applications, and especially their biophotonic applications.[13] For biophotonic applications, it is necessary that the 2PA dyes are soluble or dispersible in water, and that they remain highly fluorescent in aqueous media. Therefore, for example, with the use of in vivo imaging, these superiorities play an important role as they lead to a finer resolution, a better in-depth tissue penetration, and a decrease in cell damage.[14] Tang and co-workers recently observed a novel phenomenon that overcomes fluorescence quenching in the aggregation, which they called aggregation-induced emission (AIE). They synthesized a series of molecules such as silole, tetraphenylethene, and their derivatives, and these were induced to emit intensely by aggregate formation.[15] They also performed a series of tests to modulate, externally and internally, the restriction of the intramolecular rotation (RIR) process, which is a main cause of the AIE effect.[16] In view of this, some special 2PA dyes were designed and synthesized, which not only have a large two-photon activity, but also overcome fluorescence quenching in the aggregation. Prasad and co-workers have reported aggregation-enhanced fluorescence and two-photon absorption in nano-aggregates due to the hindering of molecular internal rotation.[17] Recently, our group designed and synthesized multibranched triarylamine end-capped triazines that exhibit enhanced 2PA and AIE properties.[18] However, there are still few reports on dyes with high 2PA and AIE.

Triphenylamine and carbazole have been widely used in opto- and electroactive materials, due to their good electron-donating and transporting capabilities, as well as their special propeller starburst molecular structure.[19] Phenothiazine is also a well-known heterocyclic compound with electron-rich sulfur and nitrogen heteroatoms, and it is a potential hole-transport semiconductor in organic devices, presenting unique electronic and optical properties.[20] Recently, 2PA materials with triarylamine as the electron donor have aroused great interest and become the focus of intensive research in this field.[10] Moreover, starburst triarylamine moieties as electron donors have better electron-donating and transporting capabilities, which may mean that the dyes have quite large two-photon activity because of the highly extended π conjugation and the appropriate intramolecular charge transfer (ICT); the introduction of the starburst triarylamine moiety is thus expected to exhibit the AIE phenomenon.[18,21] On the other hand, cyano-substituted compounds show good optical and electrical properties due to their high electron affinities. Molecules with an electron-withdrawing cyano group on the central phenylene ring are strongly fluorescent and have higher σ values.[9b] In particular, some cyano-substituted compounds have been reported which show unique enhanced emission rather than a fluorescence quenching in the solid state.[22] In this work, we connect three electron-donating dipheylamine, phenothiazine, or carbazole groups to the 1,4-positions of the benzene through bis(α-cyano-4-diphenylaminostyryl) conjugation bridges, to form three new quadrupolar-type D-π-A-π-A-π-D derivatives (**3a–c**, respectively). It could be expected that molecules with such structures containing multi-electron-donating end-cappers and cyano acceptor groups should have excellent 2PA values, as well as AIE properties.

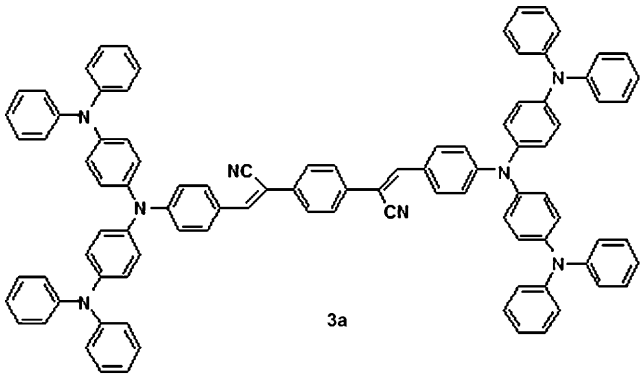

3a

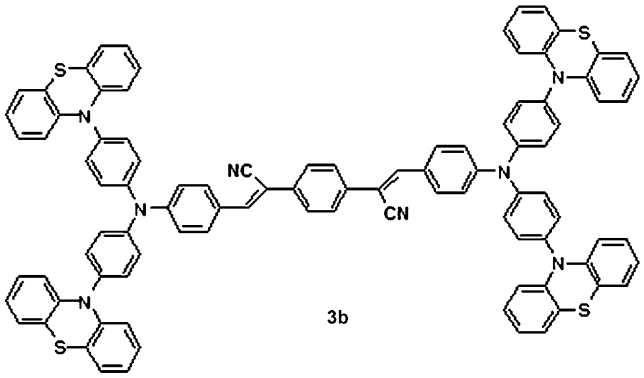

3b

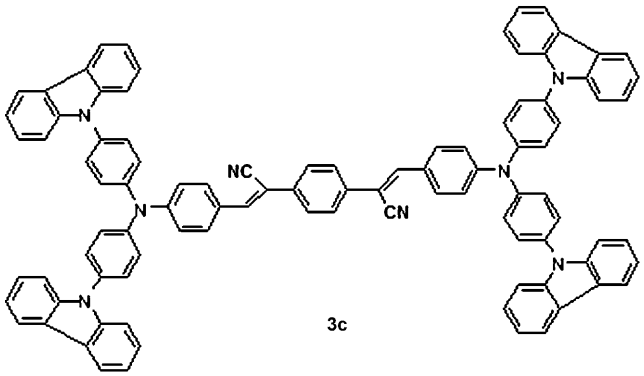

3c

Results and Discussion

Synthesis: The synthetic route to cyano-substituted diphenylamine styrylbenzene (CNDPASB)-based compounds is depicted in Scheme 1. The three dyes were prepared by a typical Knoevenagel condensation[23,24] of a triarylamine aldehyde (**2a–c**) with 2,2′-(1, 4-phenylene) diacetonitrile. The

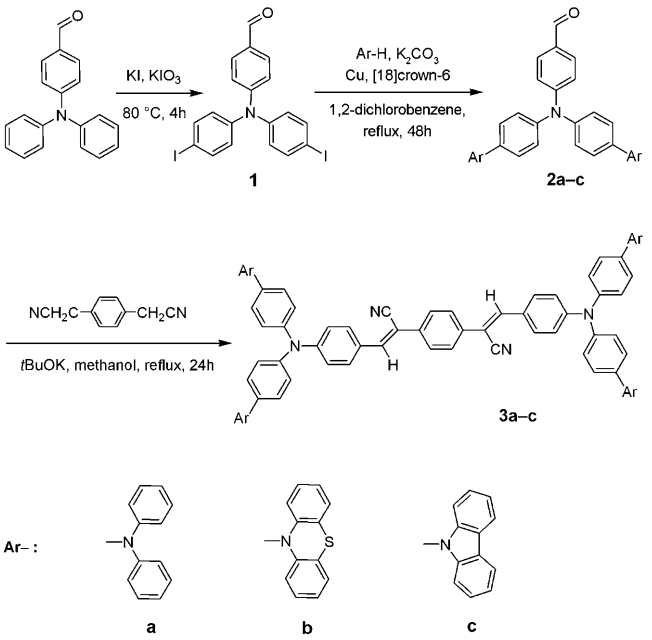

Scheme 1. Synthetic route for compounds **3a–c**.

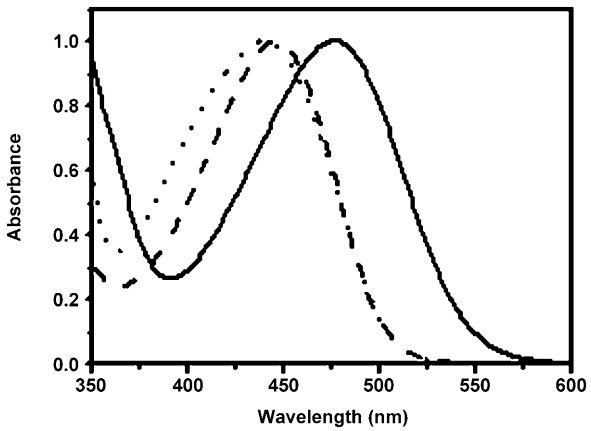

Figure 1. Normalized one-photon absorption of **3a–c** in THF: —— **3a**; – – – **3b**; ····· **3c**.

important intermediate aldehydes (**2a–c**) were readily synthesized using the Ullmann reaction between 4-[*N*,*N*-bis-(4-iodophenyl)amino]benzaldehyde (**1**) and the appropriate arylamine, that is, diphenylamine, phenothiazine, and carbazole, respectively. The molecular structure and purity of each dye were confirmed by NMR and IR spectroscopy and MS, which all gave satisfactory spectroscopic data. For example, the carbonyl signal (1690 cm^{-1}) and $-CH_2-CN$ signal (2248 cm^{-1}) were not observed on the IR spectra of CNDPASB-based derivatives, but the =C−CN signal (2208 cm^{-1}) appeared. In the ^1H NMR spectra, the signals of carbonyl groups were also not observed at about 9.90 ppm, and the signal of $-CH_2-CN$ (3.65 ppm) could not be detected, which indicated that the Knoevenagel condensation reaction had taken place. It is worth noting that the synthesis of these CNDPASB-based derivatives is very simple, and that different functional donor groups can be introduced with ease.

One-photon absorption: One-photon absorption of the dyes **3a–c** in THF at dilute concentrations are shown in Figure 1. The absorption maxima (λ_{max}) of **3a–c** are located at 473, 443, and 435 nm, respectively. It is clear that the λ_{max} of **3a** is red-shifted by 30 and 38 nm compared with those of **3b** and **3c**, respectively, which is in agreement with the order of the increase of electron-donating ability of the donors: *N*,*N*-dimethylaniline > phenothiazine > carbazole.

AIE properties: All the CNDPASB-based derivatives are soluble in common organic solvents such as THF, acetone, and dichloromethane, but are insoluble in water. Stable water dispersions of nano-aggregates of **3a–c** were prepared by the precipitation method, using THF as a water-miscible solvent for the dyes. Figure 2a shows the corresponding emission spectra of **3a** in aqueous THF with different water/THF ratios at a concentration of 1×10^{-5} M. The emission from the solution of **3a** in THF was so weak that almost no photoluminescence (PL) signal was recorded. However, solutions containing 50:50 (v/v) water/THF mixtures displayed a dramatic enhancement of red luminescence. When the water/THF ratio reached 90%, the PL intensity was boosted to the maximum. However, the spectral profile showed little change with the addition of water into a solution of **3a** in THF. Water is a not a solvent for the dye, and its molecules must aggregate in solvent mixtures with a high water content. Apparently, the emission of **3a** is induced by aggregate formation, thus verifying its AIE nature. The starburst triphenylamine is just like a rotor, and benzene is like a stator.[16] In the dilute solution, rotations of multiple triphenylamine peripheries against the benzene core may effectively deactivate its excited state nonradiatively, thus making it non-emissive. On the other hand, it is supposed that the cyano group in **3a** is effective in reducing the parallel face-to-face intermolecular interaction in the aggregated state, which consequently induces the formation of J-aggregates with enhanced fluorescence emission in the nanoparticles.[22a] Restriction of the intramolecular rotations in the aggregates blocks the channel of nonradiative decay, hence changing the dye to a strong emitter.[25] The fluorescence behavior of **3a** is well visualized through fluorescence images of the solution and nanoaggregate dispersions (see Figure 4a later). Figure 2c shows the absorption of **3a** in THF and in a dispersion of the nano-aggregate form (90% water) at 1×10^{-5} M. In contrast to the fluorescence enhancement, the absorption maximum of **3a** is red-shifted by nano-aggregation, without any notable sign of J-aggregation, implying that molecular stacking is neither too close nor well ordered within the nano-aggregated structure.[22d] The spectral red shifts indicate that planarization of the distorted conjugation is induced by aggregation, due to the intermolecular steric effect, yielding extended conjugation lengths for **3a**. Moreover, the molecules have a branched structure, which may

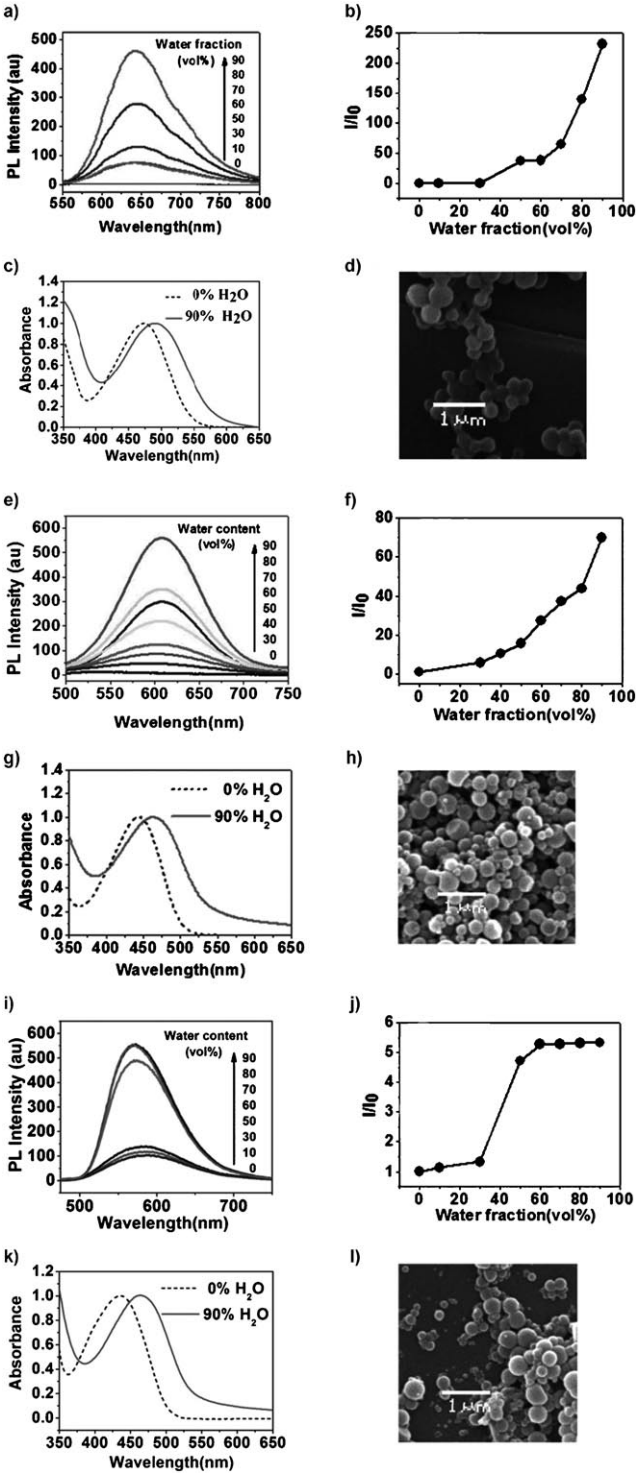

Figure 2. a), e), i) PL spectra of **3a–c**, respectively, in THF/water mixtures. b), f), j) Plots of PL peak intensity versus water content of the solvent mixture for **3a–c**, respectively. c), g), k) Absorptions of **3a–c**, respectively, in THF and in a dispersion of the nano-aggregate form (90% water) at concentrations of 1×10^{-5} M. d), h), l) SEM images of **3a–c**, respectively, nano-aggregates prepared in THF/H_2O (1:9 v/v) at concentrations of 1×10^{-5} M.

reduce the intermolecular dipole coupling because of the increased intermolecular distance in the aggregate. A representative scanning electron microscopy (SEM) image of the obtained nano-aggregates is shown in Figure 2d.

The best way to obtain a quantitative picture of the AIE process is to measure the change in the fluorescence quantum yield (Φ_F) with the variation in the amount of added water. However, such measurements are hampered by the severe light-scattering effects of the dye nano-aggregates on their absorption spectra, which makes the Φ_F determination inaccurate.[26] As an alternative, we estimated the integrals of the PL spectra, which are utilized to make the comparison. As for **3a**, there was almost no PL intensity in the solution for the 0–30% (v/v) water/THF mixture, but it started to increase swiftly upon the addition of water up to 50% (v/v). When more water is added, the dye emits more intensely, with a 230-fold increase in the I/I_0 ratio achieved at a water fraction of 90% (v/v) compared 0% (v/v) (Figure 2b). The trajectory of the I/I_0 ratio for **3a** suggests that the molecules start to aggregate at a water fraction of $>50\%$, and that the size and population of the nano-aggregates (shown in Figure 2d) continue to increase as the water fraction is increased.

Similar effects are observed for **3b**. A dilute solution of **3b** in THF gives very weak PL, but in an aqueous mixture with 90% water it emits a strong orange luminescence with a 70-fold increase in the I/I_0 ratio (Figure 2e), which means that there is an increase in nano-aggregations (Figure 2f) and that **3b** also has AIE activity. However, **3c** is different from **3a** and **3b**. Although we can detect its deep yellow fluorescence emission signal in THF, the photoluminescent intensity also increases with the addition of water into the solution of **3c** in THF. Compound **3c** exhibits aggregation-induced emission enhancement (AIEE) activity. The solution for the 50:50(v/v) water/THF mixtures displays a dramatic enhancement of luminescence. When more water is added to the dye, it emits more intensely, with a five-fold increase in the I/I_0 ratio achieved at a water fraction of 90% (v/v) (Figure 2j), suggesting that more and more nanoparticles are produced (Figure 2l). This result indicates that, by changing the triarylamine donor moiety, the CNDPASB-based compounds show AIE or AIEE performance, in which they exhibit strongly enhanced red, orange, and deep yellow fluorescence emissions.

Two-photon absorption properties: The 2PA cross sections of the **3a–c** were determined by a femtosecond open-aperture Z-scan technique, according to the method described previously.[12] Figures 3a,c,e show their data for the open-aperture Z-scan, and the 2PA coefficient obtained by data fitting. The 2PA cross section σ can be calculated by using the equation $\sigma=h\nu\beta/N_0$, in which $N_0=N_AC$ is the number density of the absorption centers, N_A is the Avogadro constant, and C represents the solute molar concentration. The values of the 2PA cross section (σ) for **3a–c** are 1016, 1484, and 814 GM, respectively, at a wavelength of 800 nm. The high 2PA properties of molecules **3a–c** are attributed to the extended π system and enhanced intramolecular charge transfer (ICT) from the triarylamine to the cyano group.

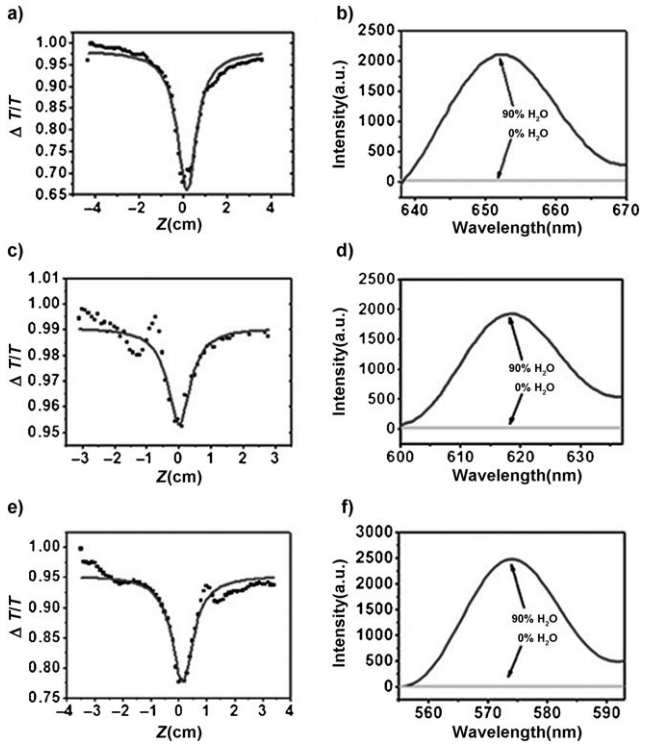

Figure 3. a), c), e) Open-aperture Z-scan traces of **3a–c**, respectively, (scattered circles are the experimental data, and the straight line is the theoretical fitted data). b), d), f) Two-photon fluorescence emission spectra for **3a–c**, respectively, in THF and in a dispersion of the nano-aggregate form (90% water) at a concentration of 1×10^{-5} M, excited at 800 nm.

Owing to the electron-donating strength (diphenylamine > phenothiazin > carbazole), the 2PA cross sections of **3a** and **3b** are much larger than that of **3c**. However, the value of **3a** is even smaller than that of **3b**, which seems to be contrary to the general conclusion that the 2PA cross section of the compound increases with electron-donating strength. This phenomenon is hard to explain at present, but may be related to the 2PA cross-section dependence on wavelength. The absorption maxima (λ_{max}) of **3a** and **3b** are located at 476 and 447 nm, respectively. The two-photon wavelength excited at 800 nm is closer to the two-fold λ_{max} of **3b**, which results in an improvement of σ. We cannot measure the 2PA cross-section profile at different wavelengths at present, because of the limit of our laser apparatus. More experiments need to be conducted to see if the 2PA cross section of **3a** is larger than **3b** at other wavelengths. This suggests that the strategy of increasing the ICT between the electron donor and acceptor is an effective approach for enhancing the 2PA cross sections of the molecules. Thus, we can control the value of the 2PA cross section to some degree by simply introducing different donors or acceptors, as required for some potential applications.

Under the excitation of an 80 fs, 800 nm pulse, **3a**, **3b**, and **3c** in a mixture of THF and water emit intense red, orange, and deep yellow fluorescence with peaks located at 651, 617, and 573 nm, respectively (Figure 3b,d,f). The good overlap between the one- and two-photon excitation fluorescence indicates that the emissions result from the same excited state, regardless of the different modes of excitation. Figures 4c,f,i show their nano-aggregates suspended in aqueous media, emitting intense red, orange, and deep yellow light, respectively, when excited with near-IR light (λ_{ex} = 800 nm) to absorb two photons.

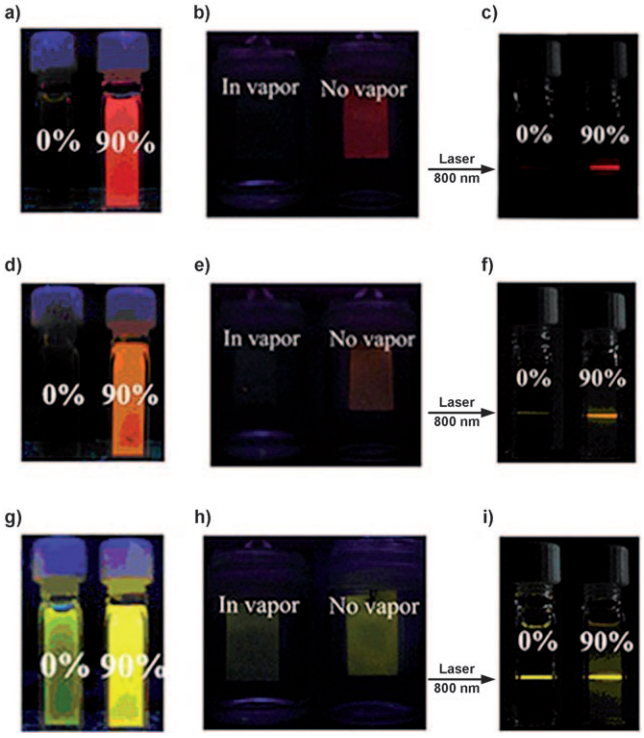

Figure 4. a), d), g) Photos of **3a–c**, respectively, in the THF/water mixtures with 0% and 90% water contents, taken under illumination with UV light. Dye concentration: 10^{-5} M; excitation wavelength: 350 nm. b), e), h) On/off fluorescence switching of **3a–c**, respectively, on TLC plates in chloroform vapor (left) and without vapor (right) under UV light (365 nm) illumination at room temperature. c), f), i) TPF emission images of **3a–c**, respectively, in the THF/water mixture (0 and 90% water).

Electrochemical properties: Figure 5 shows the cyclic voltammetry (CV) results of the compounds using 0.1 M tetrabutylammonium hexafluorophosphate as supporting electrolyte in acetonitrile, with platinum-button working electrodes, a platinum-wire counter electrode, and an SCE reference electrode. The SCE reference electrode was calibrated using the ferrocene/ferrocenium (Fc/Fc^+) redox couple as an external standard. The electrochemical properties, as well as the energy level parameters of the CNDPASB-based compounds, are listed in Table 1. As shown in Figure 5, **3a** exhibits two pairs of quasi-reversible redox peaks (0.77/0.67 and 0.93/0.86), corresponding to two triphenylamine units in different chemical environments. Compounds **3b** and **3c** each exhibit one pair of quasi-reversible redox peaks at 0.89/0.85 and 1.12/1.04, respectively. It can be speculated from Figure 5 that the first half-wave potentials (E_{ox}) of **3a–c** are 0.72, 0.87, and 1.08 V, respectively. Therefore, the

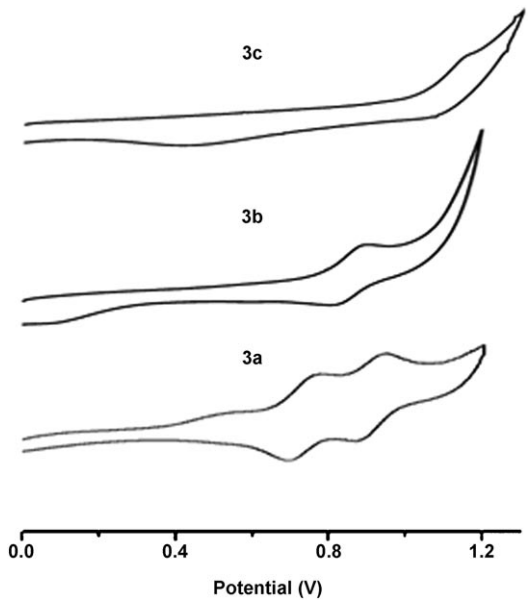

Figure 5. Cyclic voltammograms of **3a–c** in THF containing 0.1 mol L^{-1} of tetrabutylammonium hexafluorophosphate ($n$$Bu_4NPF_6$).

Table 1. Electrochemical properties of **3a–c**.

	E_{HOMO}[a] [eV]	E_{0-0}[b] [eV]	E_{LUMO}[c] [eV]	λ_{cutoff} [nm][d]
3a	−5.42	2.10	−3.42	588
3b	−5.57	2.27	−3.40	546
3c	−5.78	2.38	−3.50	520

[a] E_{HOMO} values were measured in acetonitrile with 0.1 M tetrabutylammonium hexafluorophosphate ($TBAPF_6$) as the electrolyte (working electrode: Pt; reference electrode: SCE; calibrated with ferrocene/ferrocenium (Fc/Fc+) as an external reference. Counter electrode: Pt wire). [b] E_{0-0} was estimated from the intercept of the normalized absorption and emission spectra. [c] E_{LUMO} was estimated by subtracting E_{0-0} from the HOMO. [d] Estimated from the absorption thresholds.

ground-state oxidation potential corresponding to the HOMO energy levels are −5.42, −5.57, and −5.78 eV (vs. vacuum), respectively, according to the equation HOMO = $-e(E_{ox}+4.7)$.[27] It is clear that the HOMO levels of **3a** are higher by 0.15 and 0.36 eV than those of **3b** and **3c**, respectively, which is in agreement with the order of the increase of electron-donating ability of the donors: *N,N*-dimethylaniline > phenothiazine > carbazole. Generally, a stronger electron-donating ability of the donor results in a higher HOMO energy level. It was found that the HOMO and LUMO energy levels can be tuned conveniently by changing the donor moiety, as confirmed by electrochemical measurements.

Applications of AIE materials: It is well known that AIE materials possess the on/off fluorescence switching property in some organic vapors; it is therefore suggested that one of their most important potential applications could be in the photo-switching field as a chemical vapor sensor. As shown in Figure 4b, a thin layer of **3a** developed on a TLC silica plate emits bright and deep red light under illumination with a UV lamp at room temperature. The fluorescence turns off reversibly in an atmosphere of dichloromethane vapor. This may be due to the fact that solvation of the vapor of a good solvent releases the interaction of solid molecules to a greater extent, and causes free rotation of the single bonds of the AIE molecules, leading to non-emission. The same behavior was found for **3b** (Figure 4e). However, **3c** with AIEE properties did not show this behavior (Figure 4h), so this compound may not be very suitable for on/off fluorescence switching applications.

In addition, AIE materials can also show good performances in organic light-emitting diodes (OLEDs), in which the most common materials are doped dyes. When these materials are doped in high concentrations, self-quenching of the fluorescence takes place, leading to weak luminescence which affects the performance of the OLEDs. Fortunately, AIE materials overcome the self-quenching of fluorescence in the aggregation, and have great potential for application in OLEDs.

To investigate the electroluminescent (EL) performance of those dyes, we selected **3a** and **3c**, which were made into multilayer emitting devices. Both **3a** and **3c** are used as non-doped emitters, which are made into EL devices. The detailed device architectures of the two devices are as follows: ITO/CF_x/**3a** (40 nm) or **3c** (28 nm)/TPBI (40 nm)/LiF (1 nm)/Al (100 nm), in which indium tin oxide (ITO) was used as the anode, CF_x was the hole-injection layer, the dye (**3a**/**3c**) was the light-emitting layer, TPBI (2,2′,2″-(benzene-1,3,5-triyl)-tri(1-phenyl-1*H*-benzimidazole)) was the electron-transporting layer, LiF (1 nm) was the electron-injection layer, and Al (100 nm) was used as the cathode.

The detailed EL performances of **3a** and **3c** are summarized in Table 2. A red-light emission was observed at λ_{max} = 644 nm for **3a**, with a full-width at half-maximum (FWHM) of about 100 nm, whereas **3c** showed a main EL peak at 568 nm with a FWHM of about 150 nm (Figure 6a). Compound **3c** exhibited a deep yellow emission, and the spectral profile changed little with the increase of current density (Figure 6b). Moreover, **3c** showed a good stability of the light color, whereas the performance of **3a** in this respect was worse. The current density and luminous intensity of **3a** and **3c** increased with the increase of voltage. The luminous intensity of **3c** reached 858 cd m^{-2} at ≈20 V (Figure 6c). The current efficiencies attained by the EL devices for **3a** and **3c** were 0.67 and 0.83 cd A^{-1}, respectively, equivalent to power efficiencies of 0.22 and 0.25 lm W^{-1}, respectively. The

Table 2. Performance of the EL devices made with **3a** and **3c**.

	λ[a] [nm]	V_{on}[b] [V]	η_{ext}[c]	η_c[d] [cd A^{-1}]	CIE[e] (x, y)	η_p [lm W^{-1}][f]
3a	644	10.2	0.77	0.67	(0.61, 0.38)	0.22
3c	568	9.53	0.33	0.83	(0.46, 0.50)	0.25

[a] At 20 mA cm^{-2}. [b] Turn-on voltage. [c] Maximum external quantum efficiency. [d] Maximum current efficiency. [e] CIE space values (Commission internationale de l'éclairage or International Commission on Illumination) at 20 mA cm^{-2}. [f] Maximum power efficiency.

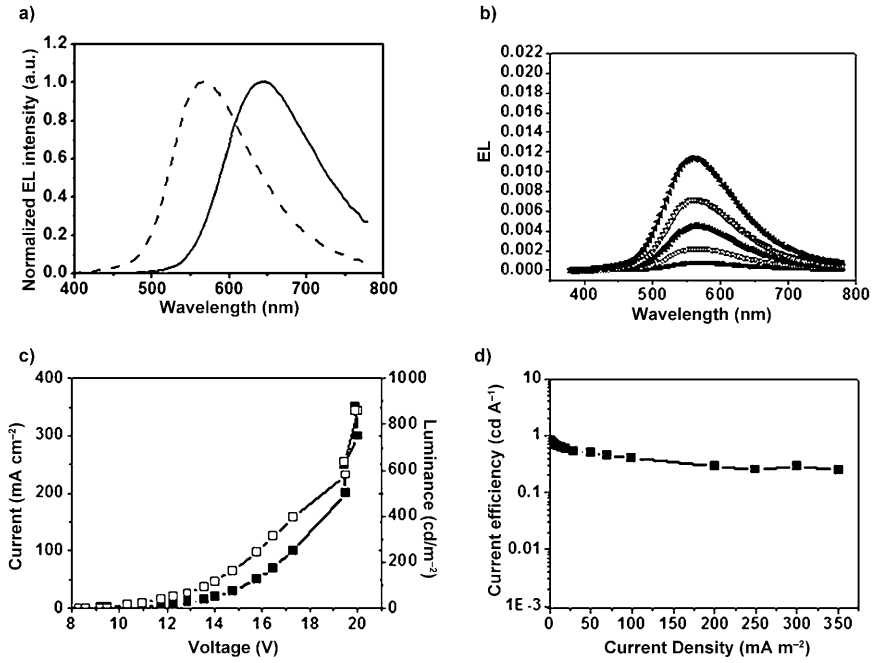

Figure 6. a) EL spectra of the devices: ——: ITO/CF_x/**3a** (40 nm) and – – –: **3c** (28 nm)/TPBI (40 nm)/LiF (1 nm)/Al (100 nm); b) EL spectra of **3c** with different current densities; ■ 5.0 mA; □ 20.0 mA; ▲ 50.0 mA; ▽ 100.0 mA; ► 250.0 mA; c) Current-density–voltage–luminance characteristics of the device: ITO/CF_x/**3c** (28 nm)/TPBI (40 nm)/LiF (1 nm)/Al (100 nm); ■ currenty density; □ luminance d) Current efficiency of **3c**.

maximum external quantum efficiencies were 0.77 and 0.33% for **3a** and **3c**, respectively (Table 2). The poor efficiencies of these two devices may be due to the imbalance of the charge carrier injection. This could also be discussed based on the energy levels of the LUMO and HOMO. The HOMO and LUMO energy levels obtained from electrochemical and UV/Vis spectra are −5.42/−3.42 and −5.78/−3.50 eV for **3a**/**3c**, respectively. The HOMO levels of the two compounds match well with the energy level of ITO glass, which would favor hole injection from the anode. However, the LUMO levels of the compounds, which act as the electron trap, would not favor electron injection. This may be why the performance of the multilayer devices was poor. Although the performance of the electroluminescence (EL) devices based on the CNDPASB derivatives reported here is only modest, a similar AIE compound used for a white EL device with high performance was recently reported by the Ma group.[28] The optimization of the OLED devices made with **3a** and **3c** is still under investigation.

Conclusions

Three new starburst triarylamine derivatives, based on cyano-substituted diphenylamine styrylbenzene (CNDPASB), **3a**–**c**, have been designed and synthesized through a concise and environmentally friendly procedure. They are non-emissive when dissolved in a "good" solvent such as THF. However, their nano-aggregates suspended in aqueous media (e.g., 9:1 v/v H_2O/THF) emit intense red, orange, and deep yellow light, respectively, when excited with near-IR light ($\lambda_{ex}=800$ nm) to absorb two photons. The result indicates that the color tuning of these CNDPASB-based compounds can be conveniently accomplished by changing the triarylamine donor moiety. The nonlinear absorption cross section of the **3b** derivative is as large as 1484 GM, so this fluorogen is a promising candidate for biosensing applications.

Experimental Section

Materials: THF was pre-dried over 4 Å molecular sieves, and distilled under an argon atmosphere from sodium benzophenone ketyl immediately prior to use. DMF was refluxed with calcium hydride and distilled before use. All other reagents and chemicals were obtained from commercial sources (J&K, Aldrich), and used without further purification.

Instrumentation: ^{1}H and ^{13}C NMR spectra were recorded on a Bruker AM-400 spectrometer using [D]chloroform as solvent and tetramethylsilane ($\delta=0$ ppm) as the internal reference. Mass spectra were recorded on an ESI mass spectrometer. FTIR spectra were recorded on a Nicolet Magna-IR550 spectrometer. The UV/Vis spectra were measured with a CARY 100 spectrophotometer. The fluorescence spectra were taken on a Varian-Cary fluorescence spectrophotometer. The cyclic voltammograms of compounds were obtained using a Versastat II electrochemical workstation (Princeton applied research), using a normal three-electrode cell with a Pt working electrode, a Pt wire counter electrode, and a regular calomel reference electrode in saturated KCl solution. The 2PA cross sections were measured by a femtosecond (fs) open-aperture Z-scan technique according to a previously described method.[12] Two-photon excited fluorescence (TPF) was achieved using femtosecond pulses with different intensities at a wavelength of 800 nm. The repetition rate of the laser pulses was 250 kHz, and the pulse duration was 80 fs.

Device fabrication: Prior to the deposition of organic materials, the indium-tin-oxide (ITO)/glass was cleaned using a routine cleaning procedure and pretreated with oxygen plasma, then coated with a polymerized fluorocarbon (CF_x) film. Devices were fabricated under about 10^{-6} Torr base vacuum in a thin-film evaporation coater following a published protocol.[29] The current–voltage–luminance characteristics were measured with a diode array rapid-scan system using a Photo Research PR650 spectrophotometer and a computer-controlled, programmable, direct-current (DC) source. All measurements were carried out in an ambient atmosphere at room temperature.

4-[*N*,*N*-Di(4-iodophenyl)amino]benzaldehyde (1): 4-(*N*,*N*-Diphenylamino)benzaldehyde (8 g, 29.3 mmol), potassium iodide (9.7 g, 58.6 mmol), acetic acid (170 mL), and distilled water (15 mL) were heated to 80 °C, with stirring maintained for 1 h. Then, potassium iodate (9.4 g, 44.0 mmol) was added and the reaction mixture was stirred for 6 h. The mixture was poured into distilled water to induce precipitation of the crude product. The precipitate was filtered off and washed with petroleum to give 12.9 g (84%) of yellow solid. ^{1}H NMR ($CDCl_3$, 400 MHz, TMS): $\delta=9.84$ (s, 1H), 7.71 (d, $J=8.0$ Hz, 2H), 7.63 (d, $J=8.0$ Hz, 4H), 7.05 (d, $J=8.0$ Hz, 2H), 6.89 ppm (d, $J=8.0$ Hz, 4H).

4-{*N*,*N*-Bis[4-(*N*,*N*-diphenylamino)phenyl]amino}benzaldehyde (2a): Compound **1** (3 g, 5.7 mmol), diphenylamine (2.9 g, 17.1 mmol), copper powder (1.6 g, 25.7 mmol), potassium carbonate (6.76 g, 49.0 mmol), and [18]crown-6 (11.1 mg, 0.042 mmol) were heated in 1,2-dichlorobenzene (100 mL) at 180 °C for 48 h under an atmosphere of argon. The inorganic components were removed by filtration after cooling. Then the solvent was distilled under reduced pressure, and the crude product was purified by column chromatography on silica (CH_2Cl_2/petroleum ether = 1:3, v/v) to give a golden yellow solid. Yield: 63 %; ^{1}H NMR ($CDCl_3$, 400 MHz, TMS): δ = () = 9.77 (s, 1 H,), 7.74 (d, J = 9.0 Hz, 2 H), 7.35 (t, J = 8.0 Hz, 8 H), 7.18 (d, J = 9.0 Hz, 4 H), 7.05–7.12 (m, 12 H), 7.03 (d, J = 9.0 Hz, 4 H), 6.92 ppm (d, J = 9.0 Hz, 2 H); MS (EI): m/z calcd calcd for $C_{43}H_{33}N_3O$ [M]: 607.3; found: 607.2.

4-{*N*,*N*-Bis[4-(*N*-phenothiazinyl)phenyl]amino}benzaldehyde (2b): Compound **1** (4 g, 7.6 mmol), phenothiazine (4.6 g, 22.8 mmol), copper powder (2.2 g, 34.2 mmol), potassium carbonate (9 g, 65.4 mmol), and [18]crown-6 (15 mg, 0.056 mmol) were heated in 1,2-dichlorobenzene (100 mL) at 180 °C for 48 h under an atmosphere of argon. The inorganic components were removed by filtration after cooling. Then the solvent was distilled under reduced pressure, and the crude product was purified by column chromatography on silica (CH_2Cl_2/petroleum ether = 1:3, v/v) to give a golden yellow solid. Yield: 50 %; ^{1}H NMR ($CDCl_3$, 400 MHz, TMS): δ = 9.88 (s, 1 H), 7.88 (d, J = 9.0 Hz, 2 H), 7.47 (d, J = 4.0 Hz, 8 H), 7.28 (d, J = 9.0 Hz, 2 H), 7.14 (d, J = 8.1 Hz, 4 H), 7.02–7.06 (m, 4 H), 6.91–6.95 (m, 4 H), 6.44 ppm (d, J = 8. 1 Hz, 4 H); MS (EI): m/z calcd for $C_{43}H_{29}N_3OS_2$ [M]: 667.2; found: 667.2.

4-{*N*,*N*-Bis[4-(*N*-carbazolyl)phenyl]amino}benzaldehyde (2c): Compound **1** (3.5 g, 6.7 mmol), carbazole (3.3 g, 20 mmol), copper powder (1.92 g, 30 mmol), potassium carbonate (8 g, 58.0 mmol), and 18-crown-6 (13 mg, 0.049 mmol) were heated in 1,2-dichlorobenzene (100 mL) at 180 °C for 48 h under an atmosphere of argon. The inorganic components were removed by filtration after cooling. Then the solvent was distilled under reduced pressure, and the crude product was purified by column chromatography on silica (CH_2Cl_2/petroleum ether = 1:3, v/v) to give a yellow–green solid. Yield: 33 %; ^{1}H NMR ($CDCl_3$, 400 MHz, TMS): δ = 9.90 (s, 1 H), 8.16 (d, J = 8.0 Hz, 4 H), 7.83 (d, J = 8.0 Hz, 2 H), 7.60(d, J=8.0 Hz, 4 H), 7.51–7.45(m, 12 H), 7.31–7.24 ppm (m, 6 H); MS (EI): m/z calcd for $C_{43}H_{29}N_3O$ [M]: 603.2; found: 603.2.

2-{4-[1-Cyano-2-(4-{*N*,*N*-bis[4-(*N*,*N*-diphenylamino)phenyl]amino}phenyl)vinyl]phenyl}-3-(4-{*N*,*N*-bis[4-(*N*,*N*-diphenylamino)phenyl]amino}-phenyl)acrylonitrile (3a): A mixture of compound **2a** (700 mg, 1.2 mmol), 2,2′-(1,4-phenylene)diacetonitrile (78 mg, 0.5 mmol), and potassium *tert*-butoxide (560 mg, 5 mmol) was dissolved in methanol (50 mL). This mixture was stirred for 24 h at reflux temperature under an atmosphere of argon. Upon cooling, a red solid precipitate was filtered off, washed with cold methanol, and purified by column chromatography on silica (CH_2Cl_2/petroleum ether = 1:1, v/v) to give a red solid. Yield: 31 %; ^{1}H NMR ($CDCl_3$, 400 MHz, TMS): δ = 7.81 (d, J = 8.2 Hz, 4 H), 7.65–7.69 (m, 4 H), 7.44–7.46 (m, 4 H), 7.26–7.29 (m, 2 H), 7.12–7.19 (m, 20 H), 7.01–7.05 ppm (m, 36 H); ^{13}C NMR ($CDCl_3$, 100 MHz, TMS): δ = 143.6, 129.9, 129.0, 128.9, 128.2, 127.9, 127.3, 127.1, 126.0, 125.8, 125.0, 124.8, 123.5, 123.3, 121.9, 120.3, 119.0, 117.4 ppm; HRMS (ESI): m/z calcd for $C_{96}H_{70}N_8$ [M]: 1334.5723; found: 1334.5768.

2-{4-[1-Cyano-2-(4-{*N*,*N*-bis[4-(*N*-phenothiazinyl)phenyl]amino}phenyl)-vinyl]phenyl}-3-(4-{*N*,*N*-bis[4-(*N*-phenothiazinyl)phenyl]amino}phenyl)acrylonitrile (3b): A mixture of compound **2b** (500 mg, 0.75 mmol), 2,2′-(1,4-phenylene)diacetonitrile (52 mg, 0.33 mmol), and potassium *tert*-butoxide (370 mg, 3.3 mmol) was dissolved in methanol (50 mL). This mixture was stirred for 24 h at reflux temperature under an atmosphere of argon. Upon cooling, an orange solid precipitate was filtered off, washed with cold methanol, and purified by column chromatography on silica (CH_2Cl_2/petroleum ether = 1:1, v/v) to give an orange solid. Yield: 30 %; ^{1}H NMR ($CDCl_3$, 400 MHz, TMS): δ = 7.86 (d, J = 8.0 Hz, 4 H), 7.63–7.68 (m, 4 H), 7.45–7.50 (m, 2 H), 7.26–7.39 (m, 20 H), 6.98–7.00(m, 10 H), 6.85–6.88 (m, 12 H), 6.77–6.81 ppm (m, 10 H); ^{13}C NMR ($CDCl_3$, 100 MHz, TMS): δ = 145.6, 144.4, 142.5, 137.7, 136.1, 132.4, 129.4, 128.7, 128.2, 127.6, 127.0, 126.6, 125.1, 124.9, 123.8, 121.7, 120.6, 120.0, 118.6, 116.6, 115.1, 113.3 ppm; HRMS (ESI): m/z calcd for $C_{96}H_{62}N_8S_4$ [M]: 1455.4059; found: 1455.4066.

2-{4-[1-Cyano-2-(4-{*N*,*N*-bis[4-(*N*-carbazolyl)phenyl]amino}phenyl)vinyl]-phenyl}-3-(4-{*N*,*N*-bis[4-(*N*-carbazolyl)phenyl]amino}phenyl)acrylonitrile-(3c): A mixture of compound **2c** (400 mg, 0.66 mmol), 2,2′-(1,4-phenylene)diacetonitrile (50 mg, 0.32 mmol), and potassium *tert*-butoxide (360 mg, 3.2 mmol) was dissolved in methanol (50 mL). This mixture was stirred for 24 h at reflux temperature under an atmosphere of argon. Upon cooling, a yellow solid precipitate was filtered off, washed with cold methanol, and purified by column chromatography on silica (CH_2Cl_2/petroleum ether = 1:1, v/v) to give a yellow solid. Yield: 37 %; ^{1}H NMR ($CDCl_3$, 400 MHz, TMS): δ = 8.17 (d, J = 8.0 Hz, 8 H), 7.91–7.97 (m, 4 H), 7.71–7.77 (m, 4 H), 7.56–7.61 (m, 8 H), 7.42–7.50 (m, 26 H), 7.25–7.33 ppm (m, 12 H); ^{13}C NMR ($CDCl_3$, 100 MHz, TMS): δ = 144.4, 139.8, 132.9, 130.1, 127.3, 125.5, 125.3, 125.0, 122.4, 119.4, 119.0, 108.8 ppm; HRMS (ESI): m/z calcd for $C_{96}H_{62}N_8$ [M]: 1327.5176; found: 1327.5167.

Acknowledgements

This work was supported by NSFC/China (20772031), the National Basic Research 973 Program (2006CB806200), the Fundamental Research Funds for the Central Universities (WJ0913001), and the Scientific Committee of Shanghai (10520709700).

[1] a) J. D. Bhawalkar, N. D. Kumar, C. F. Zhao, P. N. Prasad, *J. Clin. Laser Med. Surg.* **1997**, *15*, 201–204; b) L. L. Brott, R. R. Naik, D. J. Pikas, *Nature* **2001**, *413*, 291–293.

[2] a) D. A. Parthenopoulos, P. M. Rentzepis, *Science* **1989**, *245*, 843–845; b) J. H. Strickler, W. W. Webb, *Adv. Mater.* **1993**, *5*, 479–481; c) H. E. Pudavar, M. P. Joshi, P. N. Prasad, B. A. Reinhardt, *Appl. Phys. Lett.* **1999**, *74*, 1338–1341; d) D. Day, M. Gu, A. Smallridge, *Adv. Mater.* **2001**, *13*, 1005–1007; e) K. D. Belfield, K. J. Schafer, *Chem. Mater.* **2002**, *14*, 3656–3662; f) K. D. Belfield, Y. Liu, R. A. Negres, M. Fan, G. Pan, D. J. Hagan, F. E. Hernandez, *Chem. Mater.* **2002**, *14*, 3663–3667.

[3] a) J. D. Bhawalkar, G. S. He, C. K. Park, C. F. Zhao, G. Ruland, P. N. Prasad, *Opt. Commun.* **1996**, *124*, 33–37; b) G. S. He, R. Helgeson, T. C. Lin, Q. Zheng, F. Wudl, P. N. Prasad, *IEEE J. Quantum Electron.* **2003**, *39*, 1003–1008; c) G. S. He, T. C. Lin, V. K. S. Hsiao, A. N. Cartwright, P. N. Prasad, L. V. Natarajan, V. P. Tondiglia, R. Jakubiak, R. A. Vaia, T. J. Bunning, *Appl. Phys. Lett.* **2003**, *83*, 2733–2738.

[4] a) G. S. He, J. D. Bhawalkar, C. F Zhao, P. N. Prasad, *Appl. Phys. Lett.* **1995**, *67*, 2433–2434; b) J. E. Ehrlich, X. L. Wu, I. Y. S. Lee, Z. Y. Hu, H. Rcockel, S. R. Marder, J. W. Perry, *Opt. Lett.* **1997**, *22*, 1843–1845; c) P. L. Baldeck, Y. Morel, C. Andraud, J. F. Nicoud, A. Ibanez, *Photonics Sci. News* **1999**, *4*, 5–8; d) T. Brixner, N. H. Damrauer, P. Niklaus, G. Gerber, *Nature* **2001**, *414*, 57–60; e) J. W. Perry, J. M. Hales, S. H. Chi, J. Y. Cho, S. Odom, Q. Zhang, S. Zheng, R. R. Schrock, T. E. O. Screen, H. L . Anderson, S. Barlow, S. R. Marder, *Polym. Prepr.* **2008**, *49*, 989–990; f) K. D. Belfield, M. V. Bondar, F. E. Hernandez, O. V. J. Przhonska, *J. Phys. Chem. C* **2008**, *112*, 5618–5622; g) Y. Qian, K. Meng, C. G. Lu, B. Lin, W. Huang, Y. P. Cui, *Dyes Pigm.* **2009**, *80*, 174–180.

[5] a) W. Denk, J. H. Strickler, W. W. Webb, *Science* **1990**, *248*, 73–76; b) T. Gura, *Science* **1997**, *276*, 1988–1990; c) X. Wang, L. J. Krebs, M. AlNuri, H. E. Pudavar, S. Ghosal, C. Liebow, A. A. Nagy, A. V. Schally, P. N. Prasad, *Proc. Natl. Acad. Sci. USA* **1999**, *96*, 11081–11084; d) X. Wang, H. E. Pudavar, R. Kapoor, L. J. Krebs, E. J. Bergey, C. Liebow, P. N. Prasad, A. Nagy, A. V. Schally, *J. Biomed. Opt.* **2001**, *6*, 319–324; e) D. R. Larson, W. R. Zipfel, R. M. Williams, S. W. Clark, M. P. Bruchez, F. W. Wise, W. W. Webb, *Science* **2003**, *300*, 1434–1436.

[6] a) S. Chakrabarti, K. Ruud, *Phys. Chem. Chem. Phys.* **2009**, *11*, 2592–2596; b) S. Zein, F. Delbecq, D. Simon, *Phys. Chem. Chem. Phys.* **2009**, *11*, 694–702; c) K. A. Nguyen, P. N. Day, R. Pachter, *Theor. Chem. Acc.* **2008**, *120*, 167–175; d) C. K. Wang, P. Macak, Y. Luo, H. J. Ågren, *J. Chem. Phys.* **2001**, *114*, 9813–9820.

[7] E. Rudberg, P. Sałek, T. Helgaker, H. J. Ågren, *Chem. Phys.* **2005**, *123* 184108–1841011.

[8] M. Albota, D. Beljonne, J. L. Brédas, J. E. Ehrlich, J. Y. Fu, A. A. Heikal, S. E. Hess, T. Kogej, M. D. Levin, S. R. Marder, D. McCord-Maughon, J. W. Perry, H. Röckel, M. Rumi, G. Subramaniam, W. W. Webb, X. L. Wu, C. Xu, *Science* **1998**, *281*, 1653–1656.

[9] a) M. Rumi, J. E. Ehrlich, A. A. Heikal, J. W. Perry, S. Barlow, Z. Hu, D. McCord-Maughon, T. C. Parker, H. Röckel, S. Thayumanavan, S. R. Marder, D. Beljonne, J. L. Brédas, *J. Am. Chem. Soc.* **2000**, *122*, 9500–9510; b) S. J. K. Pond, M. Rumi, M. D. Levin, T. C. Parker, D. Beljonne, M. W. Day, J. L. Brédas, S. R. Marder, J. W. Perry, *J. Phys. Chem. A* **2002**, *106*, 11470–11480; c) M. Halik, W. Wenseleers, C. Grasso, F. Stellacci, E. Zojer, S. Barlow, J. L. Brédas, J. W. Perry, S. R. Marder, *Chem. Commun.* **2003**, 1490–1491; d) S. L. Oliveira, D. S. Corrêa, L. Misoguti, C. J. L. Constantino, R. F. Aroca, S. C. Zilio, C. R. Mendoncüa, *Adv. Mater.* **2005**, *17*, 1890–1893; e) S. J. Zheng, A. Leclercq, J. Fu, L. Beverina, L. A. Padilha, E. Zojer, K. Schmidt, S. Barlow, J. D. Luo, S. H. Jiang, A. K.-Y. Jen, Y. P. Yi, Z. G. Shuai, E. W. V. Stryland, D. J. Hagan, J. L. Brédas, S. R. Marder, *Chem. Mater.* **2007**, *19*, 432–442; f) S. J. Zheng, L. Beverina, S. Barlow, E. Zojer, J. Fu, L. A. Padilha, C. Fink, O. Kwon, Y. P. Yi, Z. G. Shuai, E. W. V. Stryland, D. J. Hagan, J. L. Brédas, S. R. Marder, *Chem. Commun.* **2007**, 1372–1374.

[10] a) G. S. He, L. S. Tan, Q. Zheng, P. N. Prasad, *Chem. Rev.* **2008**, *108*, 1245–1248; b) M. Pawlicki, H. A. Collins, R. G. Denning, H. L. Anderson, *Angew. Chem.* **2009**, *121*, 3292—3316; *Angew. Chem. Int. Ed.* **2009**, *48*, 3244–3245.

[11] G. S. He, J. Swiatkiewicz, Y. Jiang, P. N. Prasad, B. A. Reinhardt, L. S. Tan, R. Kannan, *J. Phys. Chem. A* **2000**, *104*, 4805–4810.

[12] J. L. Hua, B. Li, F. S. Meng, F. Ding, S. X. Qian, H. Tian, *Polymer* **2004**, *45*, 7143–7149.

[13] P. N. Prasad, *Introduction to Biophotonics*, Wiley-Blackwell, NY, **2003**.

[14] V. Hrobáriková, P. Hrobárik, P. Gajdo, I. Fitilis, M. Fakis, P. Persephonis, P. Zahradnik, *J. Org. Chem.* **2010**, *75*, 3053–3068.

[15] J. Luo, Z. Xie, J. W. Y. Lam, L. Cheng, H. Chen, C. Qiu, H. S. Kwok, X. Zhan, Y. Liu, D. Zhu, B. Z. Tang, *Chem. Commun.* **2001**, 1740–1741.

[16] Y. Hong, J. W. Y. Lam, B. Z. Tang, *Chem. Commun.* **2009**, 4332–4353.

[17] a) S. Kim, Q. D. Zheng, G. S. He, D. J. Bharali, H. E. Pudavar, A. Baev, P. N. Prasad, *Adv. Funct. Mater.* **2006**, *16*, 2317–2323; b) S. Kim, T. Y. Ohulchanskyy, H. E. Pudavar, R. K. Pandey, P. N. Prasad, *J. Am. Chem. Soc.* **2007**, *129*, 2669–2675.

[18] Y. H. Jiang, Y. C. Wang, J. L. Hua, J. Tang, B Li, S. X. Qian, H Tian, *Chem. Commun.* **2010**, *46*, 4689–4691.

[19] a) Z. J. Ning, H. Tian, *Chem. Commun.* **2009**, 5483–5495; b) C. Y. Chen, N. Pootrakulchote, S. J. Wu, M. Wang, J. Y. Li, J. H. Tsai, C. G. Wu, S. M. Zakeeruddin, M. Grätzel, *J. Phys. Chem. C* **2009**, *113*, 20752–20757; c) X. H. Zhang, Z. S. Wang, Y. Cui, N. Koumura, A. Furube, K. Hara, *J. Phys. Chem. C* **2009**, *113*, 13409–13415.

[20] X. P. Qiu, R. Lu , H. P. Zhou, X. F. Zhang, T. H. Xu, X. L. Liu, Y. Y. Zhao, *Tetrahedron Lett.* **2008**, *49*, 7446–7449.

[21] Z. J. Ning, Z. Chen, Q. Zhang, Y. L. Yan, S. X. Qian, Y. Cao, H. Tian, *Adv. Funct. Mater.* **2007**, *17*, 3799–3807.

[22] a) B. K. An, S. K. Kwon, S. D. Jung, S. Y. Park, *J. Am. Chem. Soc.* **2002**, *124*, 14410–14415; b) Y. P. Li, F. Li, H. Y. Zhang, Z. Q. Xie, W. J. Xie, H. Xu, B. Li, F. Z. Shen, L. Ye, M. Hanif, D. Ma, Y. G. Ma, *Chem. Commun.* **2007**, 231–233; c) B. R. Gao, H. Y. Wang, Y. W. Hao, L. M. Fu, H. H. Fang, Y. Jiang, L. Wang, Q. D. Chen, H. Xia, L. Y. Pan, Y. G. Ma, H. B. Sun, *J. Phys. Chem. B* **2010**, *114*, 128–134; d) S. B. Noh, R. H. Kim, W. J. Kim, S. Kim, K-S Lee, N. S. Cho, H-K Shim, H. E. Pudavarb and P. N. Prasad, *J. Mater. Chem.* **2010**, *20*, 7422–7429; e) B. K. An, S. H. Gihm, J. W. Chung, C. R. Park, S. K Kwon, S. Y. Park, *J. Am. Chem. Soc.* **2009**, *131*, 3950–3957.

[23] G. A. Sotzing, C. A. Thomas, J. R. Reynolds, P. J. Steel, *Macromolecules* **1998**, *31*, 3750–3752.

[24] S. C. Moratti, R. Cervini, A. B. Holmes, D. R. Baigent, R. H. Friend, N. C. Greenham, J. Gruner, P. J. Hamer, *Synth. Met.* **1995**, *71*, 2117–2120.

[25] a) Y. Q. Dong, J. W. Y. Lam, A. Qin, Z. Li, J. Sun, H. H. Y. Sung, I. D. Williams, B. Z. Tang, *Chem. Commun.* **2007**, 239–247; b) Z. Li, Y. Q. Dong, Y. H. Tang, M. Haubler, H. Tong, Y. Dong, J. W. Y. Lam, K. S. Wong, P. Gao, I. D. Williams, H. S. Kwok, B. Z. Tang, *J. Phys. Chem. B* **2005**, *109*, 10061–10066; c) Y. Q. Dong, J. W. Y. Lam, Z. Li, A. Qin, H. Tong, Y. Dong, X. Feng, B. Z. Tang, *J. Inorg. Organomet. Polym. Mater.* **2005**, *15*, 287–291; d) Y. Q. Dong, J. W. Y. Lam, A. Qin, J. X. Sun, J. Z. Liu, Z. Li, J. Z. Sun, H. Y. Sung, D. Williams, H. S. Kwok, B. Z. Tang, *Chem. Commun.* **2007**, 3255–3257.

[26] Y. Liu, X. T. Tao, F. Wang, J. Shi, J. Sun, W. Yu, Y. Ren, D. Zou, M. Jiang, *J. Phys. Chem. C* **2007**, *111*, 6544–6549.

[27] L. J. Huo, J. H. Hou, H. Y. Chen, S. Q. Zhang, Y. Jiang, T. Chen, Y. Yang, *Macromolecules* **2009**, *42*, 6564–6571.

[28] S. J. Liu, F. Li, Q. Diao, Y. G. Ma, *Org. Electron.* **2010**, *11*, 613–617.

[29] S. A. Van Slyke, C. H. Chen, C. W. Tang, *Appl. Phys. Lett.* **1996**, *69*, 2160–2161.

Received: October 1, 2010
Published online: January 24, 2011

